

# Synthesis and Phase Behavior of Cholesteric Liquid Crystal Polymers Containing Glutamic Acid in Main-Chain

Bao-Yan Zhang, Li-Feng Zhang, Mei Tian, Wen-Qiang Xiao, Yan Guan

The Centre for Molecular Science and Engineering, Northeastern University, Shenyang 110004, People's Republic of China

Received 6 October 2005; accepted 26 June 2006

DOI 10.1002/app.25027

Published online 3 July 2007 in Wiley InterScience (www.interscience.wiley.com).

**ABSTRACT:** Four polymers ( $P_0$ – $P_3$ ) containing peptide chain as polymer backbone were synthesized by condensation reaction with bis(trichloromethyl)carbonate and triethylamine. The chemical structures of the monomers  $M_0$ – $M_3$  were confirmed by FTIR and  $^1\text{H-NMR}$ . The structure–property relationships of the monomers and polymers are discussed. Their phase behavior and optical properties were investigated by differential scanning calorimetry, thermogravimetric analysis, and polarizing optical microscopy. Monomers  $M_1$ – $M_3$  and

polymers  $P_1$ – $P_3$  displayed cholesteric phases. The results demonstrated that the melt temperature and clear point of monomers ( $M_1$ – $M_3$ ) and polymers ( $P_1$ – $P_3$ ) decreased with the increase of the flexible spacer length in the side-chain, and the mesophase temperature range of the polymers increased with the increase of the flexible spacer length. © 2007 Wiley Periodicals, Inc. *J Appl Polym Sci* 106: 889–896, 2007

**Key words:** cholesteric liquid crystal polymers; glutamic acid

## INTRODUCTION

During the last decade, side-chain cholesteric liquid crystalline polymers (LCPs) have attracted considerable interest for their unique optical properties, such as selective reflection of light, thermochromism, and circular dichroism and advanced applications for instance nonlinear optical devices, full-color thermal imaging, and organic pigment.<sup>1–5</sup> Recently, many novel side-chain cholesteric LC materials have been reported.<sup>6–11</sup> The polymer backbones of side-chain LCPs are primarily polyacrylates, polymethacrylates, and polysiloxanes. There have been only a few reports on the cholesteric LCPs that take peptide chain as polymer backbones, such as PBLG, PCLG, PMLG, PEDG, PPLA, and so on.<sup>12–15</sup> As we know, the polymers containing peptide chain usually are biodegradable and biocompatible and have potential applications in numerous areas, especially in the fields of molecular biology, bionic electronics, and medicine,

etc.<sup>1,2</sup> It has been necessary to synthesize various kinds of side-chain cholesteric LCPs containing peptide chain to explore their potential applications.

In this article, four monomers containing aminoglutamic acid and their polymers containing peptide chain as backbones have been synthesized. Three of the monomers are cholesteric ones, and three of the polymers are cholesteric side-chain LCPs. The structures and properties of the monomers and the polymers have been characterized with Fourier transform infrared (FTIR), proton nuclear magnetic resonance ( $^1\text{H-NMR}$ ), differential scanning calorimetry (DSC), thermogravimetric analysis (TGA), and polarizing optical microscopy (POM). The influence of the spacer length in the side-chain of the polymers on the mesogenic properties of the polymers is discussed.

## EXPERIMENTAL

### Materials

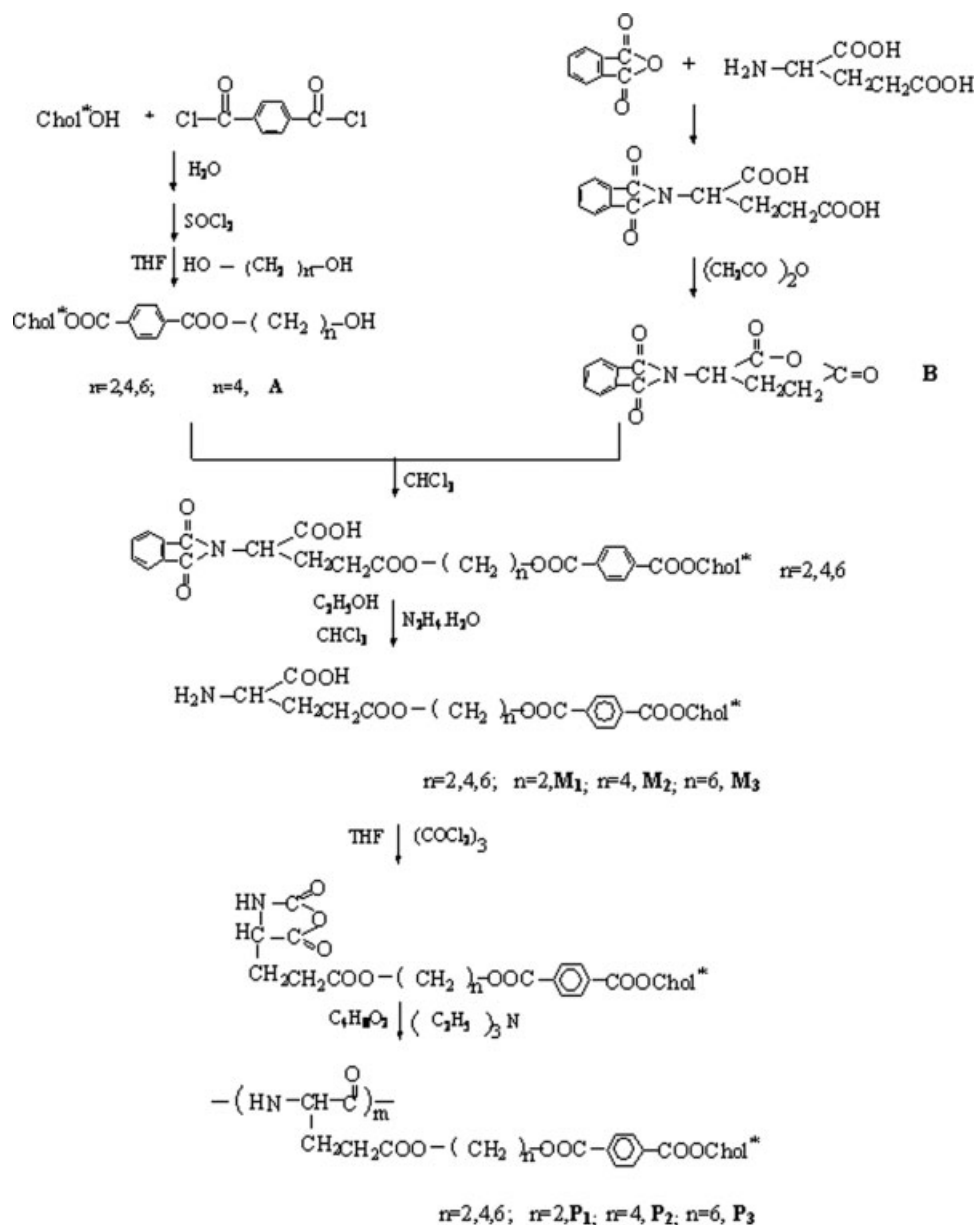
Glutamic amino acid was purchased from Shanghai Chemical Industry Company (China). Cholesterin was purchased from Henan Xiayi Medical Company (China). Tetrahydrofuran and 1,4-dioxane were first refluxed over sodium and then distilled. All other solvents and reagents were purified by standard methods.

Correspondence to: B.-Y. Zhang (byzcong@163.com).

Contract grant sponsors: National Natural Science Fundamental Committee of China, HI-Tech Research and Development Program of China, National Basic Research Priorities Program of China, Science and Technology Research Major Project of Ministry of Education of China, Specialized Research Fund.

*Journal of Applied Polymer Science*, Vol. 106, 889–896 (2007)  
© 2007 Wiley Periodicals, Inc.



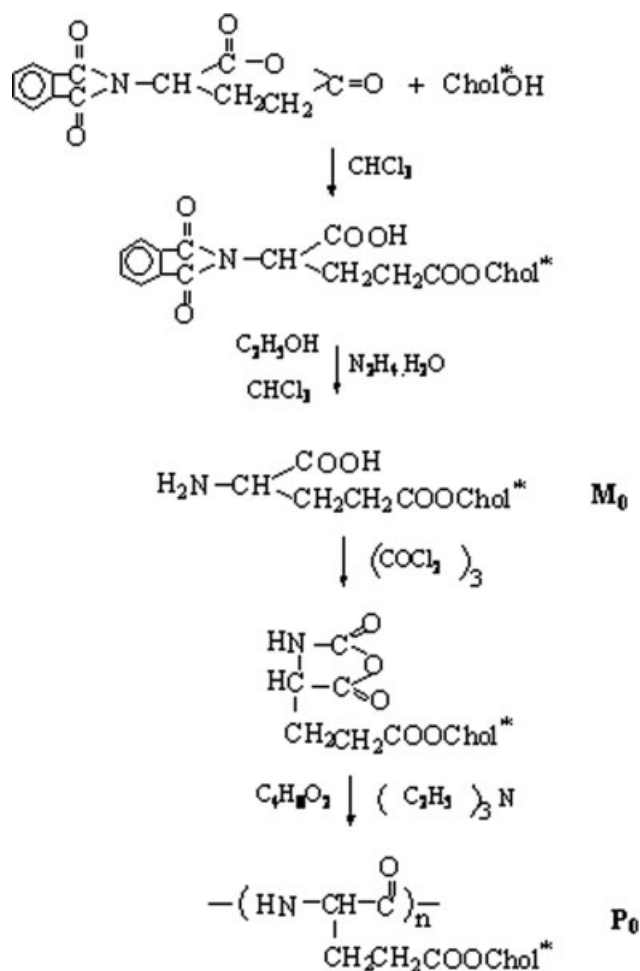


**Scheme 1** The synthesis of monomers ( $M_1$ – $M_3$ ) and polymers ( $P_1$ – $P_3$ ).

### Characterization

IR spectra were measured using a PerkinElmer spectrum (PerkinElmer Instruments, USA), as KBr pellets.  $^1\text{H-NMR}$  spectra (300 MHz) were recorded on a Varian WH-90PFT spectrometer (Varian Associates, Palo Alto, CA). Thermal transition temperatures were determined with a differential scanning calorimetry (DSC) 204 (Netzsch instruments) equipped with a liquid nitrogen cooling system at a heating and cooling rate of  $10^\circ\text{C min}^{-1}$  in a nitrogen atmosphere. The reported thermal transition temperatures were collected during the second heating cycle. The thermal stabilities of the polymers were measured with thermogravimetric analyzer using nitrogen atmos-

phere and a  $20^\circ\text{C min}^{-1}$  heating rate. A Leitz Microphot-FX (Leitz, Wetzlar, Germany) polarizing optical microscope (POM) equipped with a Mettler FP 82 hot stage and FP 80 central processor was used to observe phase transition temperature and analyze LC properties for the polymers through observation of optical textures. Dilute solution viscosity measurements were carried out in chloroform solution at  $(20 \pm 0.2)^\circ\text{C}$  using an Ubbelohde capillary viscometer. The flow times were kept sufficiently long, that is,  $>100$  s. So that kinetic energy corrections could be neglected. The optical rotations were determined with a PerkinElmer Model 341 Polarimeter. Solutions of 4 g/L in chloroform were measured in 2-mL cuv-



**Scheme 2** The synthesis of monomer ( $M_0$ ) and polymer ( $P_0$ ).

ettes of 100 mm length using light of a Na-lamp at  $\lambda = 589$  nm.

### Synthesis of the monomers

The synthetic routes to the monomers are shown in Schemes 1 and 2. The yields and structural characterization of the monomers are shown in Tables I and II.

For the synthesis of the monomers  $M_0$ – $M_3$ , the same method was adopted. The synthesis of  $M_2$  is given as an example.

### Butanediol terephthalate cholesteryl (A)

1.8 g (0.005 mol) of cholesterol in 20 mL of chloroform was added to a cold solution of 1.9 g (0.009 mol) of *p*-phthaloyl chloride in 10 mL of chloroform. The reaction mixture was heated to reflux for 15 h. The solvent was removed under reduced pressure. The crude product was washed several times by a sodium hydrogen carbonate solution, then it was neutralized to pH = 6. The precipitate was recrystallized from methanol. 5 g (0.005 mol) of the white product synthesized above and 30 mL of thionyl chloride reacted at 60°C for 3 h, and then the excess thionyl chloride was removed under reduced pressure to give the corresponding acid chloride. Then, the residual was dissolved in 10 mL of dry tetrahydrofuran, and the solution of 1.2 g (0.013 mol) of 1,4-butanediol in 20 mL of tetrahydrofuran and 0.5 mL of pyridine was added to the flask. The reaction mixture was refluxed for 20 h. The excess solvent was removed under reduced pressure. The residual was washed by water first and then was recrystallized from ethanol. The yield is 56%.

### 2-(phthalimide)-cyclopentyl acid anhydride (B)

The mixture of 1.5 g (0.01 mol) of glutamic amino acid and 1.6 g (0.011 mol) of *o*-phthalic anhydride was stirred at 180–200°C for 15 min. The mixture was recrystallized from ethanol/water (1:10) to give the corresponding protected acid. 2.3 g (0.08 mol) of the protected acid in 5 mL of acetic anhydride was stirred at 30°C for 2 h. The precipitate crude product was filtered and then washed by ether. The yield is 40%. mp: 160–161°C.

### Glutamic butanediol cholesteryl terephthalate ( $M_2$ )

1.8 g (0.007 mol) of B and 1.8 g (0.003 mol) of A in 30 mL of chloroform were heated to reflux for 72 h. The excess solvent was removed under reduced pressure. The residual was purified by recrystallization from ethanol. 4.7 g (0.005 mol) of the product synthesized earlier in 30 mL ethanol/chloroform (1 : 1) and 0.8 mL of triethylamine were stirred at 60°C for 5 h.

**TABLE I**  
Yields, Specific Rotation, and IR of Monomers

Monomer	Yield (%)	$-\alpha_{589}^{20a}$	IR (KBr) ( $\text{cm}^{-1}$ )
$M_0$	40	28.92	3220–3480(N–H,O–H),2940,2850( $\text{CH}_3,\text{CH}_2$ ),2619,2560(–COOH), 1723(C=O),1300–1100(C–O,C–N)
$M_1$	46	14.08	3200–3500(O–H,N–H),2948,2840( $\text{CH}_3,\text{CH}_2$ ),2664,2552(–COOH), 1718(C=O),1605,1512 (Ar), 1280–1120(C–O,C–N)
$M_2$	52	70.75	3180–3480(O–H,N–H),2945,2860( $\text{CH}_3,\text{CH}_2$ ),2660,2550(–COOH), 1716(C=O),1606,1510 (Ar),1280–1100(C–O,C–N)
$M_3$	43	30.25	3185–3460(O–H,N–H),2942,2856( $\text{CH}_3,\text{CH}_2$ ),2670,2558(–COOH), 1719(C=O),1608,1512 (Ar), 1260–1120(C–O,C–N)

<sup>a</sup> Measured in chloroform.

TABLE II  
 $^1\text{H-NMR}$  Results of Monomers

Monomer	$^1\text{H-NMR}$ ( $\text{CDCl}_3$ ) $\delta$ (ppm)
$M_0$	5.42 (m, 1H, $J = 8$ ppm, =CH– in cholesteryl); 4.37(m, 1H, $J = 10$ ppm, $-\text{O}-\overset{\text{H}}{\underset{\text{H}}{\text{C}}}$ in cholesteryl); 3.61 (m, 1H, $J = 8$ ppm, $\text{H}_2\text{N}-\overset{\text{H}}{\underset{\text{CH}_2-}{\text{C}}}-\text{COOH}$ ); 2.45 (m, 2H, $J = 8$ ppm, $-\text{CH}_2\text{CH}_2\text{COO}-$ ); 2.31 (m, 2H, $J = 8$ ppm, $-\overset{\text{H}}{\text{C}}-\text{CH}_2\text{CH}_2\text{COO}-$ ); 0.68–2.01 (m, 42H, in cholesteryl).
$M_1$	8.00 (s, 2H, Ar–H); 7.38 (s, 2H, Ar–H); 5.41 (m, 1H, $J = 8$ ppm, =CH– in cholesteryl); 4.61(m, 4H, $J = 8$ ppm, $-\text{OCH}_2\text{CH}_2\text{O}-$ ); 3.67(m, 1H, $J = 8$ ppm, $\text{H}_2\text{N}-\overset{\text{H}}{\underset{\text{CH}_2-}{\text{C}}}-\text{COOH}$ ); 4.36 (m, 1H, $J = 8$ ppm, $-\text{O}-\overset{\text{H}}{\underset{\text{H}}{\text{C}}}$ in cholesteryl); 2.41 (m, 2H, $J = 8$ ppm, $-\text{CH}_2\text{CH}_2\text{COO}-$ ); 2.26 (m, 2H, $J = 8$ ppm, $-\overset{\text{H}}{\text{C}}-\text{CH}_2\text{CH}_2\text{COO}-$ ); 0.69–2.03 (m, 42H, cholesteryl).
$M_2$	7.97 (s, 2H, Ar–H); 7.37 (s, 2H, Ar–H); 5.37 (m, 1H, $J = 8$ ppm, =CH– in cholesteryl); 4.88 (m, 4H, $J = 4$ ppm, $-\text{OCH}_2(\text{CH}_2)_2\text{CH}_2\text{O}-$ ); 3.74 (m, 1H, $J = 8$ ppm, $\text{H}_2\text{N}-\overset{\text{H}}{\underset{\text{CH}_2-}{\text{C}}}-\text{COOH}$ ); 4.39 (m, 1H, $J = 8$ ppm, $-\text{O}-\overset{\text{H}}{\underset{\text{H}}{\text{C}}}$ in cholesteryl); 2.47 (m, 2H, $J = 8$ ppm, $-\text{CH}_2\text{CH}_2\text{COO}-$ ); 2.25 (m, 2H, $J = 8$ ppm, $-\text{CH}_2\text{CH}_2\text{COO}-$ ); 1.54 (m, 4H, $J = 8$ ppm, $-\text{CH}_2\text{CH}_2\text{CH}_2\text{CH}_2-$ ); 0.69–2.03 (m, 42H, cholesteryl).
$M_3$	7.98 (s, 2H, Ar–H); 7.37 (s, 2H, Ar–H); 5.40 (m, 1H, $J = 8$ ppm, =CH– in cholesteryl); 4.80 (m, 4H, $J = 8$ ppm, $-\text{OCH}_2(\text{CH}_2)_4\text{CH}_2\text{O}-$ ); 3.70 (m, 1H, $J = 8$ ppm, $\text{H}_2\text{N}-\overset{\text{H}}{\underset{\text{CH}_2-}{\text{C}}}-\text{COOH}$ ); 4.37 (m, 1H, $J = 8$ ppm, $-\text{O}-\overset{\text{H}}{\underset{\text{H}}{\text{C}}}$ in cholesteryl); 2.46 (m, 2H, $J = 8$ ppm, $-\text{CH}_2\text{CH}_2\text{COO}-$ ); 2.25 (m, 2H, $J = 8$ ppm, $-\text{CH}_2\text{CH}_2\text{COO}-$ ); 1.81 (m, 4H, $J = 8$ ppm, $-\text{OCH}_2\text{CH}_2-(\text{CH}_2)_2-\text{CH}_2\text{CH}_2\text{O}-$ ); 1.42 (m, 4H, $J = 8$ ppm, $-\text{OCH}_2\text{CH}_2-(\text{CH}_2)_2-\text{CH}_2\text{CH}_2\text{O}-$ ); 0.69–2.03 (m, 42H, cholesteryl).

The excess solvent was removed under reduced pressure. The crude product was washed by methanol repeatedly. The yield is 53%, mp: 185.7°C.

### Synthesis of the polymers

For the synthesis of the polymers  $P_0$ – $P_3$ , the same method was adopted. The synthesis of  $P_2$  is given as an example.

### Synthesis of the polymer $P_2$

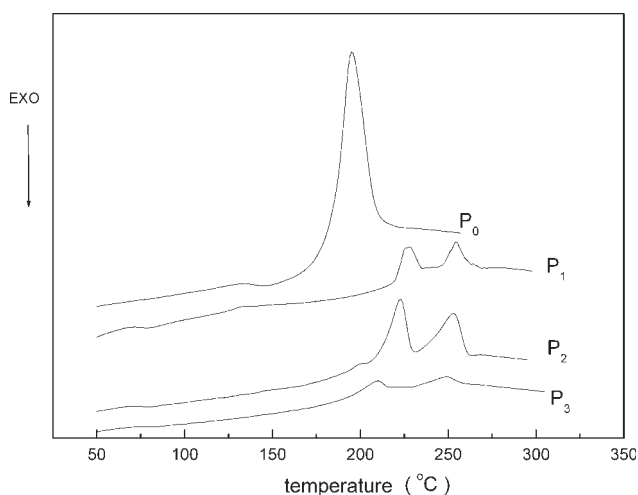
1.5 g (1.923 mmol) of  $M_2$  and 0.2 g (0.658 mol) of bis(trichloromethyl) carbonate in 220 mL of dry tetrahydrofuran was refluxed until the mixture turned clear. The reaction system was under  $\text{N}_2$  condition. Then, the solvent was removed under reduced pressure. The residual in 200 mL of 1,4-dioxane and

TABLE III  
 DSC and POM Results of Monomers and Polymers

Sample	$T_m$ (°C)	$\Delta H_m$ (J g $^{-1}$ )	$T_i$ (°C)	$\Delta H_i$ (J g $^{-1}$ )	$\Delta T$ (°C)	$T_d^a$ (°C)	LC phase
$M_0$	206.7	97.10	–	–	–	219.5	–
$M_1$	205.3	2.32	225.5	3.53	20.2	282.4	Ch <sup>b</sup>
$M_2$	185.7	5.60	220.7	3.20	35.0	241.5	Ch
$M_3$	154.5	1.53	194.5	2.33	40.0	232.1	Ch
$P_0$	194.8	46.90	–	–	–	222.5	–
$P_1$	229.2	4.10	258.2	3.30	29.0	290.9	Ch
$P_2$	222.2	6.07	254.4	4.86	32.2	276.4	Ch
$P_3$	209.5	1.08	249.0	0.96	39.5	259.6	Ch

<sup>a</sup>  $T_d$  is the 5% decomposed temperature of polymers.

<sup>b</sup> The liquid crystal texture is cholesteric.



**Figure 1** The DSC thermographs of polymers on second heating.

5 mL of triethylamine reacted at 20°C for 72 h. The product was obtained by precipitated in methanol.

IR (KBr)/cm<sup>-1</sup>: 3500–2850(N–H);1718(C=O);1605, 1516(Ar);1271(C–N);1120–1100(C–O).

## RESULTS AND DISCUSSION

### Polymerizations

The polymerization experiments are summarized in Scheme 1. The polymer molecular weight is represented by the intrinsic viscosity measured in chloroform at 20°C. The relationship between  $M_v$  and the intrinsic viscosity,  $[\eta] = kM_v^a$ , was referred to as Mark-Houwink equation. It does provide estimates for the molecular weights achieved for these polymers.

The intrinsic viscosity of  $P_0$ – $P_3$  increased with the length of the carbon chain of the side-chain in the polymers. The main reason may be the increase of molecular weight of polymers with increasing the length of the carbon chain of the side-chain in the polymers.

### Thermal analysis

The phase-transition temperatures and corresponding enthalpy changes of monomers and polymers obtained on the second heating are summarized in Table III and the DSC graphs of polymers are shown in Figure 1.

In general, the phase behavior of side chain LCPs depends on the nature of the polymer backbone, the length of the mesomorphic core, and the flexible space. The mesomorphic cores are usually attached to the polymer backbone through the flexible spacer. The polymer backbone and mesomorphic cores have antagonistic tendency, and the polymer backbone is driven toward a random coil-type configuration. The flexible spacer, which is general an aliphatic hydro-

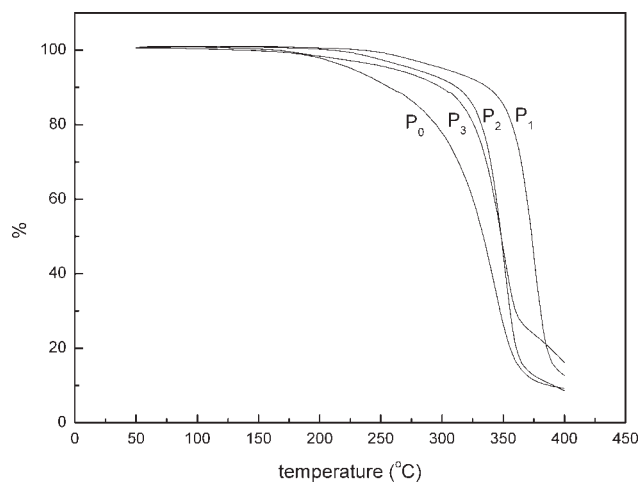


**Figure 2** The  $T_g$  thermographs of polymers.

carbon chain containing, normally, more than two methylene units decouples the mesomorphic side groups from the polymer backbone and renders the mesomorphic cores to orient-order.

The melting temperature ( $T_m$ ) and the clear point ( $T_i$ ) of  $M_0$ – $M_3$  decreased with an increase of the flexible spacer length. The phenomena also are explained as follows: with the increase of the spacer length, the molecular flexibility increases, causing a decrease of  $T_m$  and  $T_i$ . As seen from the Table III,  $T_m$  of  $M_0$  and  $M_1$  are almost the same. The reason may be that two methylene in the side-chain of  $M_1$  is not flexible enough to increase the mobility of the chain. So the decrease of  $T_m$  of  $M_1$  is slight. With the increase of the number of the methylene, the effect on the flexibility of the side chain is intense. In comparison with  $T_m$  of  $M_1$  and  $M_3$ , the number of methylene increased from 2 to 6, resulting in the decrease of  $T_m$  from 205.3°C to 154.5°C. For  $T_i$ , the similar phenomena occurred, the  $T_i$  decreased from 225.5°C to 194.5°C, when the number of methylene increased from 2 to 6.

With the increase of flexible spacer length, the  $\Delta T$  widens, that is, resulting in a wide mesomorphic temperature range.

**TABLE IV**  
Yields, Specific Rotation, and Intrinsic Viscosity of Polymers

Polymer	Yield (%)	$-\alpha_{589}^{20a}$	$[\eta]^b$
$P_0$	39	12.01	0.108
$P_1$	42	7.75	0.110
$P_2$	40	5.32	0.113
$P_3$	46	2.75	0.118

<sup>a</sup> Measured in chloroform.

<sup>b</sup> Intrinsic viscosity measured in chloroform.



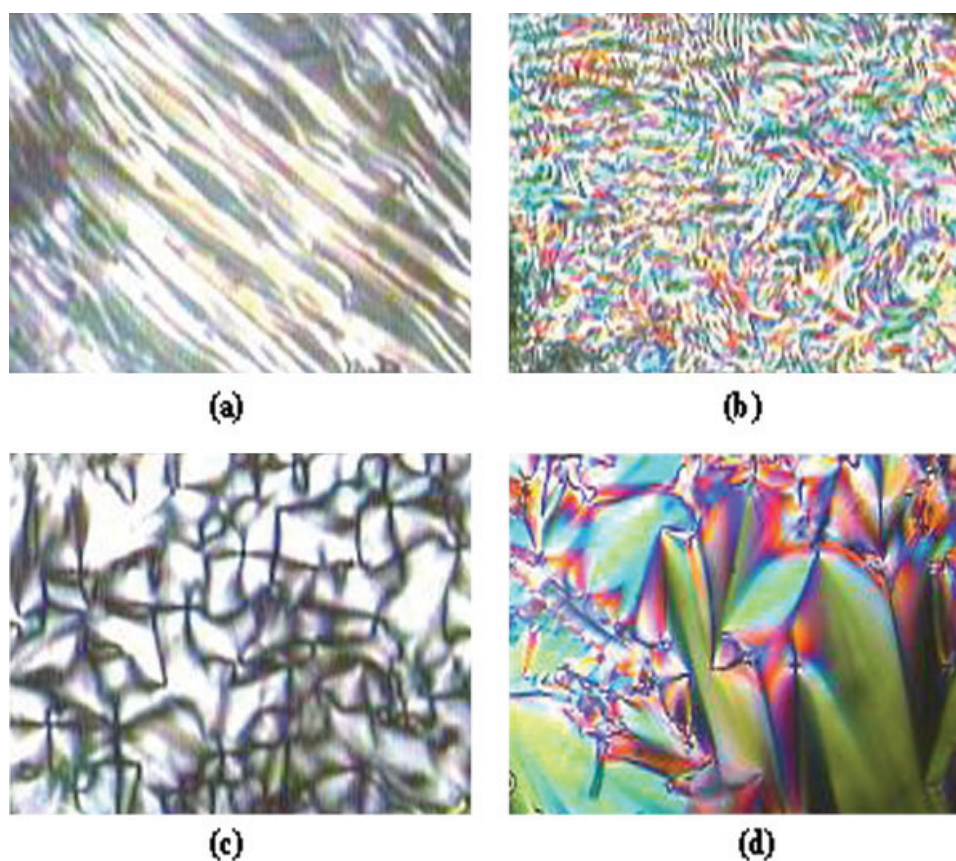


**Figure 3** Polarizing optical micrographs of monomers. (a) oily-streak texture of cholesteric of  $M_1$  on heating to 221°C; (b) helix texture of cholesteric of  $M_1$  on cooling to 213°C; (c) focal-conic texture of cholesteric of  $M_2$  on heating to 216°C; (d) focal-conic texture of cholesteric of  $M_3$  on cooling to 189°C. [Color figure can be viewed in the online issue, which is available at [www.interscience.wiley.com](http://www.interscience.wiley.com).]

The results of TGA shown in Table III and Figure 2 showed that the temperature of polymers, at which 5% weight loss occurred ( $T_d$ ), was greater than 250°C, showing that the synthesized side-chain LCPs have a higher thermal stability.

### Optical properties

All monomers and polymers synthesized are laevorotation materials. The results of specific rotation (SROT) of monomers and polymers are shown in Table I and Table IV, respectively. The SROT results demonstrated that the degree of the SROT decreased with the increase of the spacer length. The reason may be that the increasing spacer length weakened the rotating properties of the chiral molecular.

The unique optical properties of cholesteric LC are related to the helical super molecular structure of the cholesteric phase. The periodic helical structure of cholesteric phase selectively reflects visible light like a diffraction grating, whose pitch controls the wavelength of selective reflection of light. If the reflected wavelength lies in the visible range of the spectrum, the cholesteric phase exhibits brilliant colors. The transmitted light

shows a complementary color. The wavelength of selective reflection of light  $\lambda_m$  obeys the Bragg condition:

$$\lambda_m = \bar{n}p \quad (1)$$

where  $\bar{n}$  is the average index of refraction, and  $p$  is the pitch of the cholesteric phase, defined as the spatial distance over which the director rotates 360°.

Owing to the angular dependence of the reflection conditions different colors are seen depending on different observation angles. So  $\lambda_m$  is given by

$$\lambda_m = \bar{n}p \cos \theta \quad (2)$$

where  $\theta$  is the angle of incidence when  $\theta = 0^\circ$  (normal incidence).  $\lambda_m = \lambda_0 = \bar{n}p$ . The intensity of reflected light is a maximum at  $\lambda_m = \lambda_0$ , and falls off very rapidly on either side of  $\lambda_0$ .<sup>13</sup>

The helical pitch is an important parameter in connection with structures and optical properties of the cholesteric phase. It is known that the pitch and the reflection wavelength depend on the molecular structure, such as the polymers backbone, the length of mesomorphic core, flexible spacer length, and external conditions (for example, temperature, intermolec-

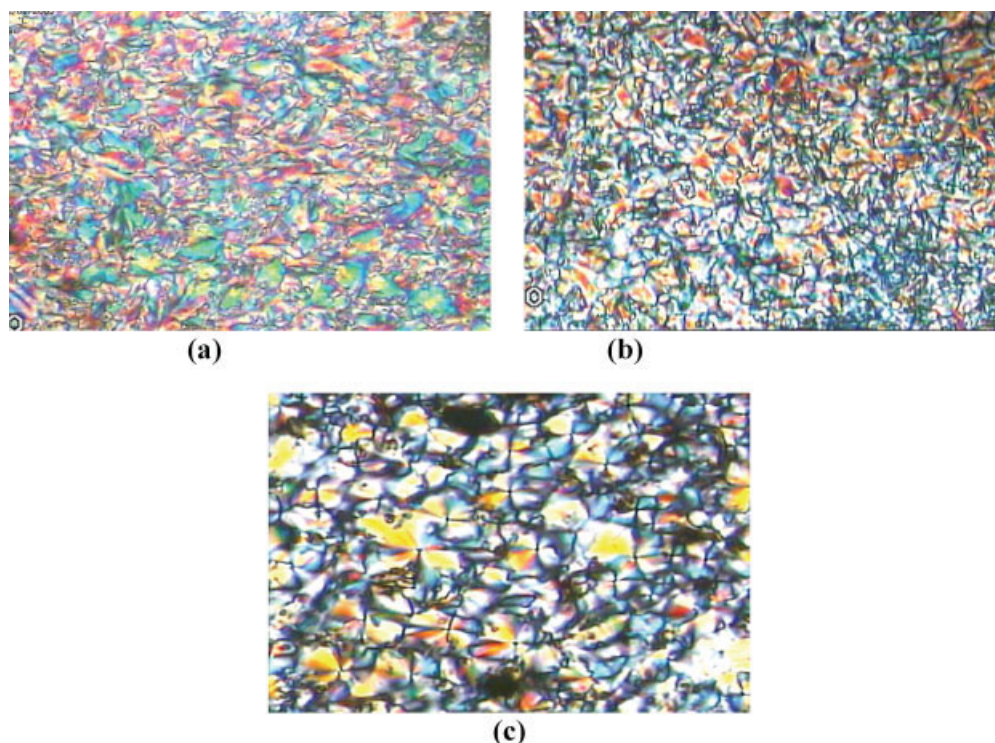


**Figure 4** Polarizing optical micrographs of polymers. (a) broken focal-conic texture of cholesteric of  $P_1$  on heating to 251°C; (b) broken focal-conic texture of cholesteric of  $P_2$  on cooling to 234°C; (c) broken focal-conic texture of cholesteric of  $P_3$  on cooling to 229°C. [Color figure can be viewed in the online issue, which is available at [www.interscience.wiley.com](http://www.interscience.wiley.com).]

ular force, electric and magnetic field). The length of flexible spacer affects not only the phase transition temperatures, but also the selective reflection wavelength of the cholesteric phase. In general, a cholesteric LC at zero field exhibits two optically contrasting stable states: planar (including oily-streak and Grandjain) and focal-conic texture. When the cholesteric phase is in the planar texture, the helical axis is perpendicular to the cell surface, and the material Bragg-reflects colored light, when cholesteric phase is in the focal-conic texture, the helical axis is forward-scattering and no selective light reflection appears.

POM results showed that the monomers  $M_1$ – $M_3$  and polymers  $P_1$ – $P_3$  exhibit oily-streak texture or focal-conic texture during heating or cooling, whereas  $M_0$  and  $P_0$  showed no texture. That may be due to their shorter flexible spacer length and greater steric hindrance of the bulky cholesteric group, which disturbed the orientation of the mesomorphic groups.

When these monomers (except for  $M_0$ ) were heated to  $T_m$ , an obvious oily-streak texture appeared. On cooling the samples from the isotropic medium, a helix texture or focal-conic was formed. Photomicrographs of  $M_1$  are shown as examples in Figures 3(a) and 3(b), and the photomicrographs of  $M_2$ ,  $M_3$  are shown in Figures 3(c) and 3(d), respectively. The polymers (except for  $P_0$ ) exhibited focal-conic texture on heating or cooling. The photomicrographs of  $P_1$ ,  $P_2$ ,  $P_3$  are shown as examples in Figures 4(a)–4(c).

The monomers ( $M_1$ ,  $M_2$ ,  $M_3$ ) all exhibited selective reflection properties. Colored reflection could be observed when they are on mesomorphic phase on heating. But no selective reflection properties of polymers were observed.

Oily-streak, focal-conic texture and selective reflection properties are the typical properties of cholesteric phase. The POM results of monomers demonstrated that  $M_1$ ,  $M_2$ ,  $M_3$  are cholesteric monomers. The POM results, DSC results, and the chemical structure of polymers demonstrated that the polymers ( $P_1$ ,  $P_2$ ,  $P_3$ ) are also cholesteric LCs.

## CONCLUSIONS

Four monomers  $M_0$ – $M_3$  and four polymers  $P_0$ – $P_3$  containing glutamic acid in main-chain were synthesized. All monomers and polymers (except for  $M_0$  and  $P_0$ ) were cholesteric phase, and exhibited oily-streak or focal-conic textures. With an increase of the flexible space length, the  $T_m$  and  $T_i$  decreased.  $M_0$  and  $P_0$  are prepared as model sample for comparison with the liquid crystal behavior of others to evaluate the effect of spacer block on liquid crystalline behavior. Three conclusions could be summarized from the results: first of all,  $M_0$  and  $P_0$  showed no liquid crystal properties, which may be due to their shorter spacer length and the greater steric hindrance of the bulky cholesteryl group disturbed the formation of the mes-

omorphous phase. Second, the increase of the flexible space length is good for forming LC phase. Finally, the range of the LC phase temperature increased with the increase of the flexible space length.

## References

1. Anne, D. M.; Etienne, S. *Macromol Chem* 1992, 193, 3031.
2. Pytela, J.; Kotva, R.; Metalova, M. *Int J Biol Macromol* 1990, 12, 241.
3. Yu, S. M.; Conticello, V. P.; Zhang, G. H. *Nature* 1997, 389, 167.
4. Lin, J. P.; Zhou, D. F. *Chem Res Chin Univ* 2000, 16, 169.
5. Kosho, H.; Tanaka, Y.; Ichizuka, T. *Polym J* 1999, 31, 199.
6. Yoshida, M.; Mitsui, S.; Nagoshi, M. *Jpn J Appl Phys Part 2* 1998, 37, 802.
7. Nakajima, A.; Hsyashi, T. *Macromolecules* 1979, 12, 840.
8. Vlasov, G. P.; Rudkovkaya, G.; Orsyannikova, L. A. *Macromol Chem* 1982, 183, 2635.
9. Tanaka, M.; Mori, A.; Imanishi, Y. *Int J Macromol* 1985, 7, 173.
10. Imanishi, Y.; Tanaka, M.; Bamford, C. H. *Int J Macromol* 1985, 7, 89.
11. Yora, R.; Hirokawa, Y.; Hayashi, T. *Eur Polym J* 1994, 30, 1397.
12. Chen, J. B.; Jeong, Y. I.; Cho, C. S. *Polymer* 1999, 40, 2041.
13. Das, P.; Xu, J.; Roy, J. *J Chem Phys* 1999, 111, 8240.
14. Wang, L. G.; Huang, Y. *Chin J Cell Sci Tech* 2000, 8, 7.
15. Dong, Y. M.; Yuan, Q.; Xiao, Z. L. *Chem J Chin Univ* 1999, 20, 140.